Robot-Assisted Image-Guided Targeting for Minimally Invasive Neurosurgery: Planning, Registration, and In-vitro Experiment

R. Shamir[1], M. Freiman[1], L. Joskowicz[1], M. Shoham[2,3], E. Zehavi[3], and Y. Shoshan[4]

[1] School of Eng. and Computer Science, The Hebrew Univ. of Jerusalem, Israel
[2] Dept. of Mechanical Engineering, Technion, Haifa, Israel
[3] Mazor Surgical Technologies, Caesarea, Israel
[4] Dept. of Neurosurgery, School of Medicine, Hadassah University Hospital, Israel
josko@cs.huji.ac.il

Abstract. This paper present a novel image-guided system for precise automatic targeting in keyhole minimally invasive neurosurgery. The system consists of a miniature robot fitted with a mechanical guide for needle/probe insertion. Intraoperatively, the robot is directly affixed to a head clamp or to the patient skull. It automatically positions itself with respect to predefined targets in a preoperative CT/MRI image following an anatomical registration with a intraoperative 3D surface scan of the patient facial features. We describe the preoperative planning and registration modules, and an in-vitro registration experiment of the entire system which yields a target registration error of 1.7mm (std=0.7mm).

1 Introduction

Precise targeting of tumors, lesions, and anatomical structures with a probe or a needle inside the brain based on preoperative CT/MRI images is the standard of care in many keyhole neurosurgical procedures. The procedures include tumor biopsies, catheter insertion, deep brain stimulation, aspiration and evacuation of deep brain hematomas, and minimal access craniotomies. Additional procedures, such as tissue and tumor DNA analysis, and functional data acquisition, are rapidly gaining acceptance and also require precise targeting. These minimally invasive procedures are difficult to perform without the help of support systems that enhance the accuracy and steadiness of the surgical gestures.

Four types of support systems for keyhole neurosurgery are currently in use: 1. stereotactic frames; 2. interventional imaging systems; 3. navigation systems, and; 4. robotic systems. Stereotactic frames provide precise positioning with a manually adjustable frame rigidly attached to the patient skull. These extensively used frames provide rigid support for needle insertion, and are relatively accurate and inexpensive ($< 1mm$, USD 50K). However, they require preoperative implantation of frame screws, head immobilization, and manual adjustment during surgery. They cause patient discomfort and do not provide real-time validation. Interventional imaging systems produce images showing the actual needle

J. Duncan and G. Gerig (Eds.): MICCAI 2005, LNCS 3750, pp. 131–138, 2005.
© Springer-Verlag Berlin Heidelberg 2005

position with respect to the predefined target [1,2,3]. Their key advantage is that they account for brain shift. A few experimental systems also incorporate optical real-time tracking and robotic positioning devices. However, their nominal and operational costs are high and their availability is very limited. Furthermore, brain shift is a secondary issue in keyhole neurosurgeries.

Navigation systems (e.g., Medtronic, USA and BrainLab, Germany) show in real time the location of hand-held tools on the preoperative image onto which targets have been defined [4,5,6]. Augmented with a manually positioned tracked passive arm (e.g., Phillips EasyTaxis^{TM}), they also provide mechanical guidance for targeting. While these systems are now in routine clinical use, they are costly (USD 250K), require head immobilization and maintenance of line-of-sight for tracking, and additional time for registration and manual arm positioning.

Robotic systems provide frameless stereotaxy with a robotic arm that automatically positions itself with respect to a target defined in the preoperative image [7,8,9,10]. Registration between the image and the intraoperative situation is done by direct contact or with video images. Two floor-standing commercial robots include NeuroMate^{TM} (Integrated Surgical Systems, USA) and PathFinder^{TM} (Armstrong HealthCare, UK). Their advantages are that they are rigid, accurate, and provide a frameless integrated solution. However, since they are bulky, cumbersome, and costly (US 300K), they are not commonly used.

2 System Overview and Protocol

We are developing a novel image-guided system for precise automatic targeting of structures inside the brain that aims at overcoming the limitations of existing solutions [11]. The system automatically positions a mechanical guide to support keyhole drilling and insertion of a needle or probe based on predefined entry point and target locations in a preoperative CT/MRI image. It incorporates the miniature MARS robot (Mazor Surgical Technologies) [12,14], originally developed for orthopaedics, mounted on the head immobilization clamp or directly on the patient skull via pins (Fig. 1). Our goal is a robust system for keyhole neurosurgical procedures which require clinical accuracy of 1–1.5mm.

The key idea is to establish a common reference frame between the preoperative CT/MRI image and the intraoperative patient head and robot locations with an intraoperative 3D surface scan of the patient's facial features. Once this registration has been performed, the transformation that aligns the planned and actual robot targeting guide location is computed. The robot is then automatically positioned and locked in place so that its targeting guide axis coincides with the entry point/target axis.

The system hardware consists of: 1) the MARS robot and its controller; 2) a custom robot mounting base, targeting guide, and registration jig; 3) an off-the-shelf 3D surface scanner, and; 4) a standard PC. MARS is a $5 \times 8\text{cm}^2$ cylinder, 250–gram six-degree-of-freedom parallel manipulator with workvolume of about 10cm^3 and accuracy of 0.1mm. It operates in semi-active mode; when locked, it is rigid and can withstand lateral forces of up to 10N [13]. The adjustable robot

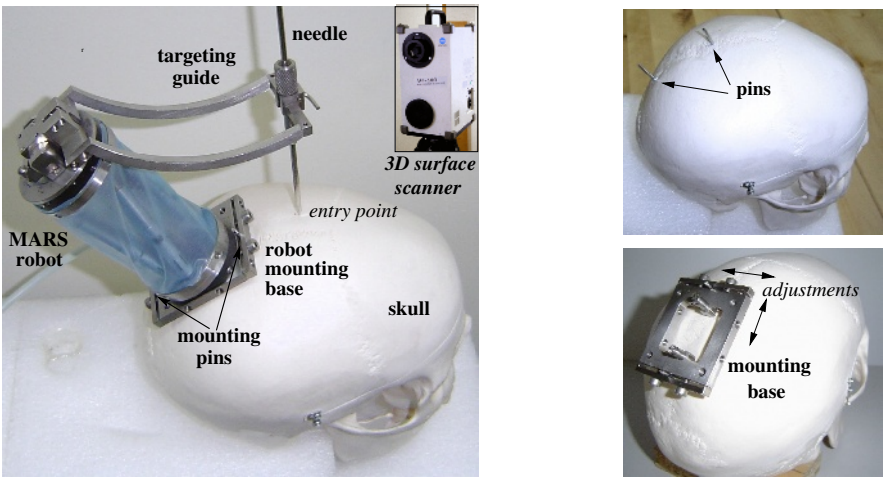

Fig. 1. The MARS robot mounted on the skull

mounting jig attaches the robot base to either the head immobilization frame or to skull-implanted pins. The system software modules are: 1) preoperative planning; 2) intraoperative execution; 3) surface scan processing; and 4) three-way registration. This paper describes the first and last modules.

The surgical protocol is as follows. A preoperative marker- and frame-less CT/MRI image of the patient is acquired. Next, with the preoperative planning module, the surgeon defines on the image the entry points and target locations, and determines the robot mounting type (head clamp or skull) and the desired robot location. Intraoperatively, guided by a video-based intraoperative module, the surgeon places the robot approximately in its planned location. When the robot is mounted on the head frame, the robot base is attached to an adjustable mechanical arm affixed to the head clamp. When mounted on the skull, two 4mm pins are screwed under local anesthesia on the skull and the robot mounting base is attached to them. Next, the registration jig is placed on the robot mounting base and a surface scan showing both the patient forehead and the registration jig is acquired. The registration jig is then replaced by the robot with the targeting guide on it, and the registration module automatically computes the offset between the actual and the desired targeting guide orientation. It then positions and locks the robot so that the actual targeting guide axis coincides with the planned needle insertion trajectory. On surgeon demand, the system automatically positions the robot for each of the predefined trajectories.

3 Preoperative Planning

The preoperative planning module inputs the CT/MRI image and geometric models of the robot, its workvolume, and the targeting guide. It automatically builds from the CT/MRI image the face surface and extracts four landmarks

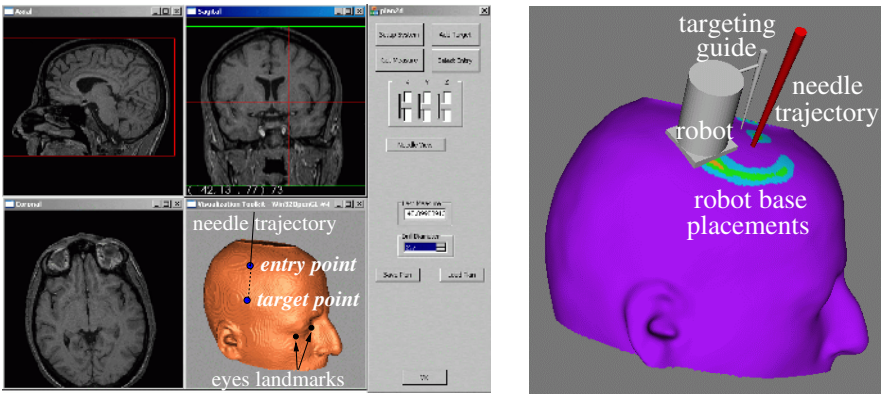

(a) entry and target point selection (b) robot base location and range

Fig. 2. Preoperative planning module screens

near the eyes to be used later for coarse registration. The module allows interactive visualization of the CT/MRI slices and the face surface, and enables the surgeon to define entry and target points and visualize the resulting needle trajectories (Fig 2a). Based on the surgeon-defined entry and target points, and the robot mounting mode (on the skull or on the head clamp), the module computes a suggested preferred approximate robot base placement and its range. The computed robot base placement is such that the needle trajectories are at the center of the robot work volume. Placements away from it are assigned a score based on how far they are from the robot work volume center. The results are graphically shown to the surgeon (Fig 2b), who can then select the approximate actual position to satisfy clinical criteria, such as avoiding placements near the cranial sinuses, temporal muscle, or emissary vein. The output includes the surgical plan (entry and target points), the approximate robot base placement, and the patient face surface mesh and landmarks.

The algorithm for computing and rating the robot placements proceeds as follows. A needle trajectory is associated with a coordinate frame whose z axis is aligned with the needle axis and points towards the target. For each point on a uniform $5 \times 5\text{mm}^2$ grid of possible robot base placements over the skull, the rigid transformation that aligns the targeting guide z axis, held by the robot in its home position, with the needle trajectory axis, is computed based on Horn's closed-form solution. The robot base location is then computed by composing the fixed transformation from the targeting guide to the robot top, and the transformation from the robot top to the robot base. The resulting robot transformation is scored against the robot home position based on their distance.

4 Registration

The three-way registration module computes the transformation that establishes a common reference frame between the preoperative CT/MRI, the robot mount-

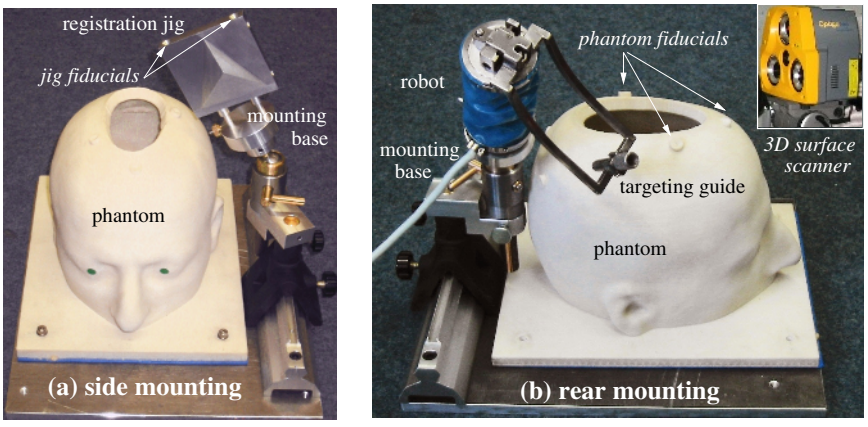

(a) front view, with registration jig (b) side view, with robot

Fig. 3. In-vitro experimental setup

ing base, and the intraoperative patient situation. Two transformations are computed to this end: CT/MRI to intraoperative patient face and robot mounting base to intraoperative patient face. The module inputs the intraoperative surface scans of the registration jig and of the patient's face, and four eye landmarks from the 3D surface scan processing module.

The transformation between the face surface scanner cloud of points and the corresponding CT/MRI surface is performed by first computing a coarse correspondence between them from the extracted landmark eye points in both datasets. This correspondence is then refined with robust Iterative Closest Point (ICP) registration [15], which is performed between a small (1,000–3,000) subset of the surface scan points and the CT/MRI points on the face/ear surface.

The transformation between the robot mounting base and the patient face is performed with a custom-designed registration jig. The registration jig is a $75 \times 75\text{mm}^2$ base with a wide-angled tetrahedron of 9mm height that is placed on the robot mounting base (Fig 3a). It is designed so that all four planes can be seen from a wide range of scanning viewpoints, with sufficient area for adequate scan sampling. To facilitate plane identification, all pairwise plane angles are different. The registration jig model is matched to the surface scanner data as follows. First, we compute a Delaunay triangulation of the registration jig scanner cloud of points. Next, the normals of each mesh triangle are computed and classified into five groups according to their value: four groups correspond to each one of the planes of the registration jig, and one to noise. A plane is then fitted to the points in each of the groups, and four points, corresponding to the intersection between any three planes, are computed. The affine transformation between these four points and the corresponding ones in the model is then computed. Finally, an ICP rigid registration on the plane points is computed to further reduce the error. The actual robot mounting base location with respect to the preoperative plan is determined from this transformation, and from it and the robot characteristics, the targeting guide location.

5 Experimental Results

We have implemented a complete hardware and software prototype of the proposed system and designed an in-vitro registration experiment to validate it. In earlier work [11], we measured the accuracy of the MRI/surface scan registration by acquiring 19 pairs of MRI/3D surface scans of the first two authors with different facial expressions – worried or relaxed, eyes open or closed. The MRI scans are $256 \times 256 \times 200$ pixels^3 with voxel size of $0.93 \times 0.93 \times 0.5$mm^3 from which 100,000-150,000 face surface points are extracted. The surface scans were obtained with a laser scanner (Konica Minolta Vivid 910, USA – accuracy of 0.1mm or better). The registration RMS error was 1.0mm (std=0.95mm) computed in 2 secs, which is adequate and compares favorably with [16].

In this in-vitro registration experiment of the entire system, we manufactured the registration jig, a positionable robot mounting base, and a precise stereolithographic phantom replica of the outer head surface of the second author from an MRI dataset (Fig 3). Both the phantom and the registration jigs include fiducials for contact-based registration. The phantom is attached to a base with a rail onto which slides a manually adjustable robot mounting base.

To verify the accuracy of the three-way registration algorithm, we used an optical tracking system (Polaris, Northern Digital, Canada – 0.3mm accuracy) to measure the relative locations of the phantom and the registration jig. Their spatial location was determined by touching with a calibrated tracked pointer the phantom and registration jig fiducials. The phantom and the registration jig were scanned with a video scanning system (Optigo200, CogniTens – 0.03mm accuracy). We then computed two registration chains (Fig 4), and measured the

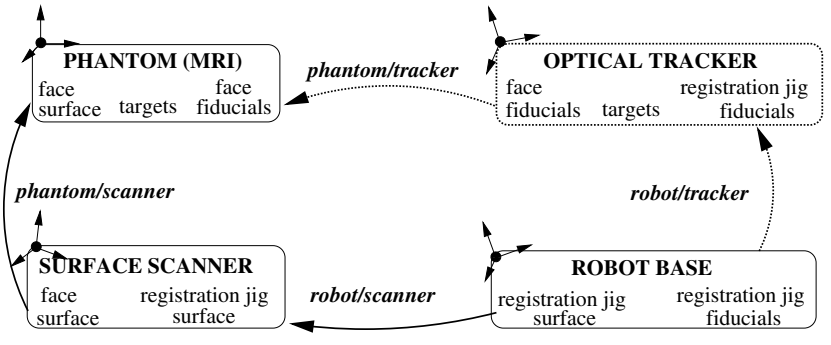

Fig. 4. Registration chains for in-vitro experiment. Each box corresponds to an independent coordinate system. The location of the phantom targets with respect to the robot base origin is computed once via the surface scanner (phantom/scanner and robot/scanner transformations) using the face and registration face surfaces, and once via the optical tracker (phantom tracker and robot/tracker transformations) using the registration jig and the face fiducials. By construction, the phantom and the MRI are in the same coordinate system.

Table 1. In-vitro registration results (in mm) of five experiments. The 2nd and 3rd are the surface scanner phantom and robot base surface registration errors. The 4th and 5th column are the fiducial tracker phantom and registration jig registration errors (both FRE – Fiducial Registration Error – and TRE – Target Registration Error for a target at about 150mm from the mounting base. The 6th column is the error between the target scanner and tracker fiducial locations.

Set	**phantom/scan** RMS (std)	**robot/scan** RMS (std)	**phantom/tracker** FRE (TRE)	**robot/tracker** FRE (TRE)	**Error** (std)
1.	0.45 (0.16)	0.31 (0.22)	0.50 (0.61)	0.71 (0.68)	2.71
2.	0.46 (0.17)	0.28 (0.20)	0.50(0.61)	0.71 (0.68)	1.85
3.	0.46 (0.17)	0.25 (0.13)	0.22 (0.53)	0.65 (0.69)	1.31
4.	0.46 (0.18)	0.34 (0.27)	0.22 (0.53)	0.65 (0.69)	1.09
5.	0.44 (0.14)	0.21 (0.08)	0.76 (0.79)	0.73 (0.73)	1.49
Avg.	0.46 (0.17)	0.28 (0.18)	0.44 (0.62)	0.67 (0.69)	1.69 (0.7)

location error of phantom targets with respect to the robot mounting base as computed by the surface scanner and the optical tracker.

Table 1 shows the results of five experiments. The Target Registration Error (TRE) is 1.7mm, which is close to the desired clinical goal. It includes the positional error tracked pointer tip, estimated at 0.5mm (this can be improved with a more accurate measuring system). In addition, we measured the accuracy of the registration between the real faces and the CogniTens scans, taken several months apart, as we did in the earlier experiment. The RMS error is 0.7mm (std=0.25mm), which shows that registration based on facial features is accurate and stable over time. We also measured the accuracy of the robot and registration jig mounting with the optical tracker by putting on and off 10 times the registration jig and measuring the fiducial offset location. The FRE is 0.36mm (std=0.12mm), which is within the measuring error of the optical tracker.

6 Conclusion

We have described a system for automatic precise targeting in minimally invasive keyhole neurosurgery that aims at overcoming the limitations of the existing solutions. The system, which incorporates the miniature parallel robot MARS, will eliminate the morbidity and head immobilization requirements associated with stereotactic frames, eliminate the line-of-sight and tracking requirements of navigation systems, and provide steady and rigid mechanical guidance without the bulk and cost of large robots. This paper presents the preoperative planning and registration modules, and the first results on an in-vitro registration experiment. It establishes viability of the surface scan concept and the accuracy of the location error of phantom targets with respect to the robot base to 1.7mm, which is close to the required 1–1.5mm clinical accuracy in many keyhole neurosurgical procedures.

Acknowledgments. This research is supported in part by a Magneton grant from the Israel Ministry of Industry and Trade. We thank Dr. Tamir Shalom and CogniTens for their generous assistance in acquiring the scans, ad Haim Yeffet for manufacturing the experimental setup platform.

References

1. Tseng, C-S. Chen, H-H. Wang, S-S, et al., "Image guided robotic navigation system for neurosurgery". *Journal of Robotic Systems* **17**(8), 2000, pp 439-447.
2. Chinzei, K. Miller. K. "MRI Guided Surgical Robot". *Australian Conf. on Robotics and Automation*, Sydney, 2001.
3. Kansy, K. Wikirchen, P. Behrens, U. et al. "LOCALITE - a frameless neuronavigation system for interventional magnetic resonance imaging". *Proc. of Medical Image Computing and Computer Assisted Intervention*, 2003, pp 832-841.
4. Kosugi, Y. Watanabe, E. Goto, J. et al. "An articulated neurosurgical navigation system using MRI and CT images". *IEEE Trans. on Biomedical Eng.* **35**(2), 1998.
5. Akatsuka, Y. Kawamata, T. Fujii, M. et al. "AR navigation system for neurosurgery". *Proc. of Medical Imaging and Computer-Aided Interventions*, 2000.
6. Grimson, E, Leventon, M. Ettinger, G. et al., "Clinical experience with a high precision image-guided neurosurgery system". *Proc. of Medical Imaging and Computer-Aided Interventions*, 1998, pp 63-72.
7. Chen, MD. Wang, T. Zhang, QX et al.,"A robotics system for stereotactic neurosurgery and its clinical application". *Proc. Conf. Robotics and Automation*, 1998.
8. Masamune, K. Ji, LH. Suzuki, M. et al., Takeyoshi Dohi, Hiroshi Iseki, "A newly developed stereotactic robot with detachable drive for neurosurgery". *Proc. of Medical Image Computing and Computer Aided Imaging*, 1998, pp. 215-222.
9. Davies, B. Starkie, B. Harris, S. et al. "Neurobot: a special-purpose robot for neurosurgery", *Proc. Int. Conf. and Robotics and Automation*, 2000, pp 410-414.
10. Hang, Q. Zamorano, L. Pandya, A. et al., "The application of the NeuroMate Robot: a quantitative comparison with frameless and frame-based surgical localization systems". *Computer Aided Surgery* **7**(2), 2002, pp 90-98.
11. Joskowicz, L. Shoham, M. Shamir, R. Freiman, M. Zehavi, E. and Shoshan, Y. "Miniature robot-based precise targeting system for keyhole neurosurgery: concept and preliminary results". *19th Int. Conf. on Computer-Assisted Radiology and Surgery*, CARS'2005, H.U. Lemke et. al. editors, Elsevier 2005, to appear,
12. Shoham, M. Burman, M. Zehavi, E. et al., "Bone-mounted miniature robot for surgical procedures: concept and clinical applications". *IEEE Trans. on Robotics and Automation* **19**(5), 2003, pp 893-901.
13. Wolf, A. Shoham, M. Schinder M. and Roffman, M. "Feasibility study of a mini robotic system for spinal operations: analysis and experiments", *European Spine Journal*, 2003.
14. Yaniv, Z. and Joskowicz, L. "Registration for robot-assisted distal locking of long bone intramedullary nails", *IEEE Trans. on Medical Imaging*, to appear, 2005.
15. Besl, P.J. and McKay, N.D. "A method for registration of 3D shapes", *IEEE Trans. on Pattern Analysis and Machine Intelligence*, **14(2)**, 1992.
16. Marmulla, R. Hassfeld, S. and Lueth, T. "Soft tissue scanning for patient registration in image-guided surgery", *Computer-Aided Surgery* **8**(2), 2003, pp70-81.